NMR Solution Structure of an α-Bungarotoxin/Nicotinic Receptor Peptide Complex[†,‡]

Vladimir J. Basus,[§] Guoqiang Song,[∥] and Edward Hawrot*,[⊥]

Department of Pharmaceutical Chemistry, University of California, San Francisco, California 94143, Shanghai Institute of Materia Medica, Academia Sinica, Shanghai, China 200031, and Section of Molecular and Biochemical Pharmacology, Division of Biology and Medicine, Brown University, Providence, Rhode Island 02912

Received June 10, 1993; Revised Manuscript Received August 27, 1993[⊛]

ABSTRACT: We report the two-dimensional nuclear magnetic resonance (NMR) characterization of the stoichiometric complex formed between the snake venom-derived long α-neurotoxin, α-bungarotoxin (BGTX), and a synthetic dodecapeptide (α185–196) corresponding to a functionally important region on the α-subunit of the nicotinic acetylcholine receptor (nAChR) obtained from *Torpedo californica* electric organ tissue. BGTX has been widely used as the classic nicotinic competitive antagonist for the skeletal muscle type of nAChR which is found in the avian, amphibian, and mammalian neuromuscular junction. The receptor dodecapeptide (α185–196) binds BGTX with micromolar affinity and has been shown to represent the major determinant of BGTX binding to the isolated α-subunit. Previous studies involving covalent modification of the native nAChR from *Torpedo* membranes with a variety of affinity reagents indicate that several residues contained within the dodecapeptide sequence (namely, Tyr-190, Cys-192, and Cys-193) apparently contribute directly to the formation of the cholinergic ligand binding site. The NMR-derived solution structure of the BGTX/receptor peptide complex defines a relatively extended conformation for a major segment of the "bound" dodecapeptide. These structural studies also reveal a previously unpredicted receptor binding cleft within BGTX and suggest that BGTX undergoes a conformational change upon peptide binding. If, as we hypothesize, the identified intermolecular contacts in the BGTX/receptor peptide complex describe a portion of the contact zone between BGTX and native receptor, then the structural data would suggest that α-subunit residues 186–190 are on the extracellular surface of the receptor.

Ligand-gated ion channels represent a large, evolutionarily related group of intrinsic membrane proteins that form multisubunit complexes and transduce the binding of small agonists into transient openings of ion channels. The first requisite step in channel activation is the binding of the agonist to select receptor determinants which are then believed to trigger a subtle conformational rearrangement leading to channel opening. The nicotinic acetylcholine receptor (AChR) is the prototypic ligand-gated cation-selective channel, and the availability of high-affinity antagonists, the α-neurotoxins, has greatly facilitated the biochemical and molecular characterization of this receptor/channel complex (Stroud et al., 1990; Galzi et al., 1991). The snake venom α-neurotoxins such as α-bungarotoxin (BGTX) competitively block or occlude the binding of agonists to the AChR. A major determinant of the antagonist binding site, which likely overlaps the agonist binding site, is thought to reside on the α-subunit between residues 173 and 204 on the basis of the following observations. Small synthetic peptides corresponding to this region bind BGTX (Wilson et al., 1985, 1988; Neumann et al., 1986a,b; Ralston et al., 1987; Gotti et al., 1987; Radding et al., 1988; Conti-Tronconi et al., 1990; Tzartos & Remoundos, 1990), and AChRs from BGTX-resistant animals and from neuronal AChRs which are insensitive to BGTX contain altered sequences within this region [e.g., Barchan et al., (1992)]. Studies with synthetic peptides and recombinant fusion proteins are in general agreement in localizing the key residues responsible for BGTX binding to the region that contains residues 181–198 (Wilson et al., 1985, 1988; Neumann et al., 1986a,b; Aronheim et al., 1988; Radding et al., 1988). The shortest peptide retaining high binding activity for BGTX is the heptapeptide α189–195 (Tzartos & Remoundos, 1990). The BGTX-binding dodecapeptide corresponding to residues 185–196 of the *Torpedo* α-subunit binds BGTX, in solution, with an apparent K_d of 1.4 μM (Pearce et al., 1990), in good agreement with other binding studies (Neumann et al., 1986a,b; Aronheim et al., 1988; Wilson et al., 1988). Synthetic peptide analogue studies and site-directed mutagenesis of recombinant proteins suggest that residues Tyr-189 and Tyr-190 play an important function in BGTX binding (Gotti et al., 1988; Tzartos & Remoundos, 1990; Pearce et al., 1990; Ohana et al., 1991; Conti-Tronconi et al., 1991; Chaturvedi et al., 1992).

The 173–204 region of the α-subunit also plays a significant role in agonist recognition as indicated by covalent labeling studies with [^{3}H]-4-(*N*-maleimido)-α-benzyltrimethylammonium, which place Cys-192 and Cys-193 (*Torpedo* numbering) within the agonist binding site (Kao et al., 1984). Cys-192 and Cys-193, in the native receptor, form a highly unusual vicinal disulfide with great potential for conformational rearrangement in response to agonist binding (Kao & Karlin, 1986). This disulfide is not, however, required for BGTX binding (Tzartos & Remoundos, 1990; McLane et al., 1991; Schlyer et al., 1992). Many other spectroscopic, covalent labeling, and site-directed mutagenesis studies provide additional evidence that residues in the α181–198 region

† This work was supported by an NSF grant (DMB9104794) to V.J.B. and an NIH grant (GM32629) to E.H.

‡ All coordinates, distance constraints, and dihedral angles for the structure of the complex will be deposited in the Brookhaven Protein Data Bank.

* Address correspondence to this author.

§ University of California.

∥ Academia Sinica.

⊥ Brown University.

⊛ Abstract published in *Advance ACS Abstracts,* November 1, 1993.

0006-2960/93/0432-12290$04.00/0

contribute to agonist binding (Mishina et al., 1985; Dennis et al., 1988; Abramson et al., 1989; Fraenkel et al., 1990; Middleton & Cohen, 1991; Tomaselli et al., 1991; Galzi et al., 1991a,c; O'Leary & White, 1992; Pearce and Hawrot, manuscript in preparation).

The α-neurotoxin family of proteins has been widely and extensively studied over the last 25 years [reviewed in Endo and Tamiya (1987)], providing a great deal of structural information. The structure–function analysis to date has been largely based on (1) the comparison of conserved sequences among over 60 identified and characterized α-neurotoxins, (2) chemical modification studies, and (3) the X-ray crystal structures of three α-neurotoxins (Low et al., 1976; Tsernoglou et al., 1978; Walkinshaw et al., 1980; Love & Stroud, 1986; Betzel et al., 1991). BGTX is a relatively flat, hand-shaped protein with overall dimensions of 40 Å × 30 Å × 20 Å. As modification of no single residue appears to eliminate receptor binding, it has been suggested that toxin/receptor binding involves a multipoint attachment (Endo & Tamiya, 1987). Although a number of amino acid residues have been implicated in receptor recognition, there has been very little direct evidence to reveal the molecular mechanism underlying receptor binding and specificity. Electron microscopy (Kistler et al., 1982), small-angle X-ray diffraction studies (Fairclough et al., 1983), and electron image analysis of BGTX bound to AChR-enriched membranes (Kubalek et al., 1987) suggest that BGTX lies atop the synaptic crest of the receptor at positions corresponding to the two α-subunits and may protrude some distance into the central vestibule. The localization of BGTX astride the synaptic crest is consistent with fluorescence energy-transfer experiments indicating that at least a portion of bound α-toxin resides near the outer perimeter of the receptor (Johnson et al., 1984) and that a receptor region interacting with an α-toxin residue located midway along the 40-Å length of the toxin is itself about 40 Å above the plane of the membrane (Herz et al., 1989). These findings suggest that the tip of the middle α-neurotoxin loop cannot extend any closer than 20 Å to the membrane bilayer (Herz et al., 1989).

NMR structural data (Basus et al., 1988) indicate that the solution structure of BGTX, while consistent with the X-ray structures of α-cobratoxin and erabutoxin (Low et al., 1976; Walkinshaw et al., 1980; Corfield et al., 1989), is different in several key respects from the X-ray structure of BGTX (Love & Stroud, 1986). Several other members of the α-neurotoxin family have been studied by NMR (Endo et al., 1981; Inagaki et al., 1985; Labhardt et al., 1988; Yu et al., 1990; Oswald et al., 1991; Sutcliffe et al., 1992; Le Goas et al., 1992; Zinn-Justin et al., 1992). A common goal in these studies has been the identification of structural features important for nicotinic receptor recognition and specificity. NMR structure determinations have been carried out on about 100 proteins of up to 157 amino acids in length (Bax, 1989; Wagner et al., 1992) and are now being extended to the study of protein complexes where short synthetic peptides can be used to reveal the important features of binding domains important for protein recognition (Ikura et al., 1992).

In this study we have prepared the complex formed between the dodecapeptide *Torpedo* α185–196, containing the Cys-192–Cys-193 disulfide, and BGTX to determine the three-dimensional structure of the complex using two-dimensional (2-D) NMR techniques. The structure of the complex provides fundamentally important information on the molecular configuration and localization of several key residues in the dodecapeptide as they exist in the toxin-bound state. In addition, we have identified a number of residues in BGTX that are perturbed upon binding and which suggest a major site of molecular recognition mediating toxin binding to the α-subunit of the AChR.

MATERIALS AND METHODS

Synthetic Peptide Preparation. Solid-phase peptide synthesis and HPLC purification of the α185–196 dodecapeptide KHWVYYTCCPDT was performed by the Yale Protein and Nucleic Acid Chemistry Facility, New Haven, CT. As the 2-D NMR studies required high concentrations of complex, we prepared the internal disulfide (Cys-192–S–S–Cys-193) form of the dodecapeptide to preclude any possibility of thiol–disulfide reaction between the two peptide cysteines and the five disulfides in BGTX. The oxidation was carried out by the slow addition of a dilute dodecapeptide solution to a slight molar excess of potassium ferricyanide solution at neutral pH (Rivier et al., 1978; Gray et al., 1984). The extent of reaction was determined by the Ellman color reaction with DTNB (Ellman, 1959). Unreacted dodecapeptide in the sulfhydryl form was removed by passing the reaction mixture through an Affi-Gel-501 organic mercurial resin (Bio-Rad) according to the manufacturer's specifications. The reaction mixture was then lyophilized and desalted and the oxidized dodecapeptide isolated by preparative C18 reverse-phase HPLC. Upon analytical C18 HPLC with an acetonitrile gradient and 0.1% trifluoroacetic acid in the aqueous phase, the single peak of oxidized dodecapeptide migrates at the same position as the reduced dodecapeptide except that the peak is much broader. The purified oxidized dodecapeptide was unreactive with DTNB and with the sulfhydryl-modifying reagent *N*-ethylmaleimide, as determined by analytical HPLC, and thus was free of the reduced dodecapeptide. Typically, yields were about 50%. The predicted molecular weight of the purified disulfide–peptide (1513.6) was confirmed by mass spectrometry. Binding competition studies with native AChR were performed as described previously (Pearce et al., 1990) and indicated that the K_d of the disulfide–dodecapeptide for BGTX is 3 μM.

Cys-192 and Cys-193 are normally linked by a disulfide in the membrane-bound native AChR (Kao et al., 1986), and the redox state of this Cys pair in the native receptor has little effect (<3-fold) on α-neurotoxin binding affinity (Hamilton et al., 1985). 1-D and 2-D ^{1}H NMR studies of the complex formed between the thiol form of the dodecapeptide and BGTX indicate that perturbations in BGTX chemical shifts are similar with both peptide preparations, consistent with the finding that the disulfide is not essential for binding of BGTX to the dodecapeptide. With the disulfide form of the dodecapeptide we were able to carry out NMR studies of the complex at high concentrations (5 mM) and elevated temperatures (45 °C), conditions under which there is some precipitation with the free sulfhydryl form of the peptide.

Two-Dimensional NMR and Structure Calculation. For 2-D NMR, the complex was prepared in 95% H_2O–5% D_2O, pH = 5.8. The reference "free" BGTX assignments at pH 5.8 were obtained by examining the previously identified chemical shifts of cross-peaks in the NOESY and HOHAHA spectra at pH 4.0 (Basus et al., 1988) and by following the incremental changes in resonance positions upon the stepwise adjustment of the pH first to 5.0 and finally to 5.8. We observed no major change in the structure of free BGTX between pH 4.0 and pH 5.8.

The ROESY (rotating frame NOESY) NMR experiment (Bothner-By et al., 1984; Bax & Davis, 1985) was carried out at 45 °C; ^{1}H frequency = 500 MHz; ROESY mixing time = 100 ms; acquired data size, 512 × 2048; 16 scans per t_1

increment. In ROESY experiments of this sort, NOE cross-peaks are of opposite sign and were not plotted. Some of the cross-peaks in the ROESY spectra of the same sign as the chemical exchange cross-peaks are due to intramolecular *J*-coupling between neighboring protons (e.g., in the Gln side chain $-NH_2$) and were identified by comparing the HOHAHA spectra of free BGTX with the HOHAHA spectra of the complex.

NOESY NMR experiments were carried out at 15, 25, 35, and 45 °C; ^1H frequency = 500 MHz; NOESY mixing time = 150 ms; acquired data size, 512 × 2048; 16 scans per t_1 increment. All reported chemical shifts are relative to an internal standard [sodium 3-(trimethylsilyl)propionate] included in all samples.

Representative solution structures of the complex formed between BGTX and the first six amino acids of the dodecapeptide were computed in two stages and were based on 365 BGTX constraints (146 long range, 155 sequential, 64 dihedral angles) and the intermolecular constraints shown in Table III. In the first stage of computation, a distance geometry calculation was carried out using the Cray Y-MP at the San Diego Supercomputer Center with the program VEMBED, a vectorized version of EMBED (Havel et al., 1983; Kuntz et al., 1989). In the second stage, the structures produced by distance geometry were adjusted by restrained molecular dynamics (rMD) and energy minimizations performed with the GROMOS-87 programs (van Gunsteren & Berendsen, 1987) using a SUN Sparc2 workstation. For all calculations, *in vacuo* conditions were assumed and all charged groups were neutralized. The 37D4 force field was applied in these calculations, and the SHAKE algorithm (van Gunsteren & Berendsen, 1987) was used to keep all bond lengths constant. The distance restraint K_{dis} was increased linearly from 0.6 to 10 kcal/(mol·Å^2) in the first 3 ps, while the temperature was kept at 600 K followed by 2 ps at 600 K with K_{dis} = 10 kcal/(mol·Å^2). The time constant t_{tc} for coupling to the thermal bath was set to 0.2 ps for the first 5 ps of the rMD runs and was set to 2 ps for the next 6 ps where the temperature was allowed to drop (final temperature setting was 0 K). The long time constant was used to avoid trapping in local energy minima as the temperature is lowered in the annealing phase of the rMD calculations (Gippert et al., 1990). The final temperatures at the end of the 11-ps dynamics run were in the range of 200–300 K. The structures generated by rMD were then energy minimized using K_{dis} = 10 kcal/(mol·Å^2). As a result of four independent structural calculations, the average root mean square deviation between all pairs of structures was 1.7 Å for the receptor/peptide backbone atoms. For the entire complex, an average root mean square deviation of 2.6 Å was obtained for the backbone atoms excluding the previously described, poorly constrained BGTX regions involving residues 30–38 and 69–74 (Basus et al., 1988).

RESULTS

Stoichiometry of Binding and Suitability for 2-D NMR Analysis. Figure 1 shows the effect of varying the molar ratio of dodecapeptide to BGTX on an identifiable resonance (the CδH of His-4 in BGTX) in a 1-D NMR spectrum. We found that the chemical shift position of the His-4 CδH imidazole ring proton in BGTX is altered upon complex formation and consequently binding and the stoichiometry of the complex can be monitored by following the disappearance of the His-4 CδH resonance. Incremental addition of dodecapeptide to BGTX resulted in a steady diminution of the CδH resonance corresponding to free BGTX and the appearance of three new resonances in this region (Figure 1).

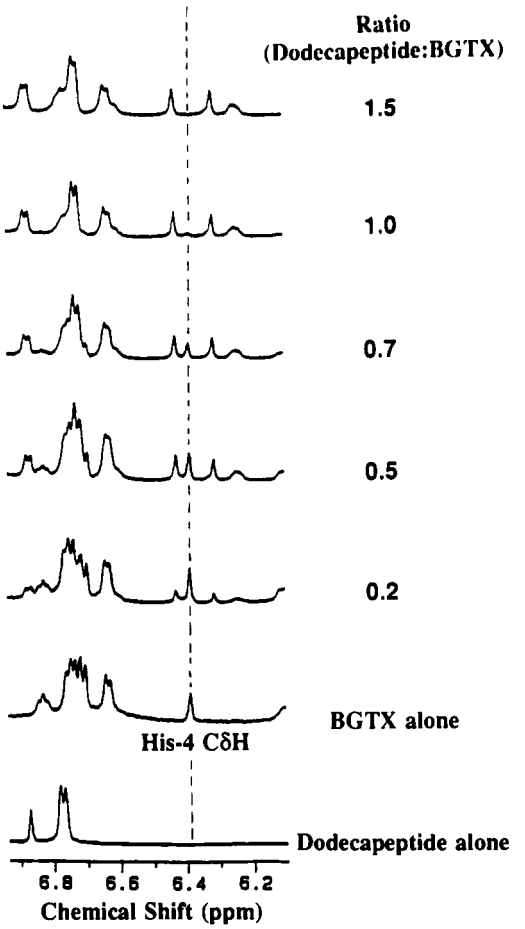

FIGURE 1: Stoichiometry of binding determined by varying the molar ratio of BGTX and dodecapeptide. One-dimensional NMR spectra were obtained in D_2O on mixtures of BGTX and dodecapeptide as indicated. Samples were incubated in 20 mM sodium phosphate buffer, pH 8.3 at 25 °C, for 24 h. BGTX concentrations ranged from 0.5 to 1.0 mM, and the dodecapeptide concentrations ranged from 0.2 to 1.0 mM. The complete assignment of the BGTX resonances has been carried out at pH 4 (Basus et al., 1988), and the pH dependence of the His-4 CδH proton shift is known (Endo et al., 1981), so that the position of the CδH resonance of His-4 in BGTX (Figure 1) is unambiguous. The dashed line indicates the chemical shift position of the His-4 CδH resonance in free BGTX. The fully reduced peptide was used in this experiment, but similar results were seen with the disulfide form of the peptide and at the pH used for the 2-D NMR studies (pH 5.8).

We have assigned these three resonances (see below), and they correspond to protons in the complexed ("bound") form of BGTX. From left to right in Figure 1, the three new resonances in the stoichiometric complex that lie between chemical shift 6.5 ppm and 6.2 ppm correspond to (1) CδH of His-68, (2) CδH of His-4, and (3) CαH of Met-28 (the broadest of the three resonances). At an equimolar concentration of dodecapeptide and BGTX (0.5 mM each; i.e., 160-fold above the apparent K_d for the disulfide form of the dodecapeptide as determined in this study), the resonance corresponding to the CδH of His-4 in free BGTX is abolished, indicating that the stoichiometry of the complex is 1:1. Furthermore, the 1:1 stoichiometry indicates that the synthetic dodecapeptide is homogeneous in its capability to bind BGTX.

The incremental decrease in the CδH resonance of His-4 in free BGTX and the concomitant increase in the new resonances corresponding to bound BGTX indicate that the complex exists in slow chemical exchange with free BGTX at 45 °C. The apparent rate of exchange between free and bound forms of BGTX is $\leq \sim 0.5\ s^{-1}$ at 45 °C on the basis of the slow exchange peaks of His-4 CδH.

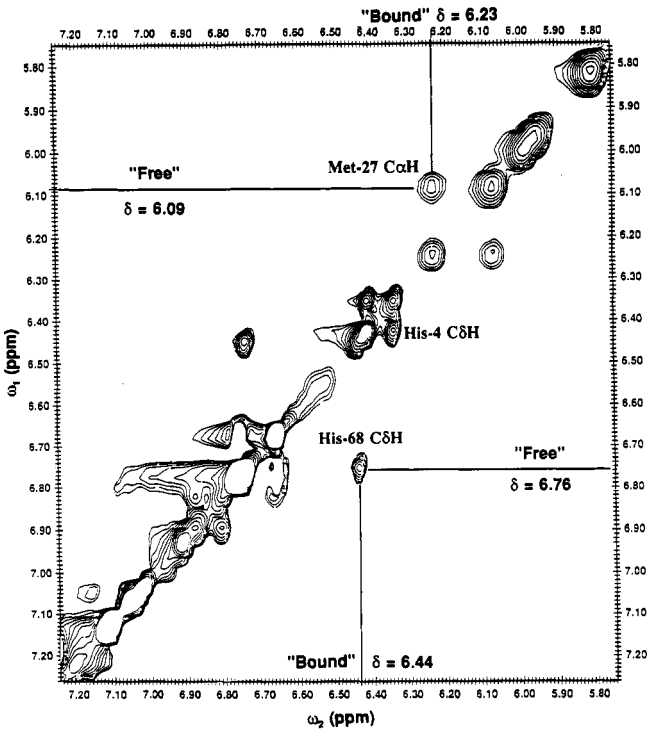

FIGURE 2: Chemical exchange cross-peaks used for assignment of bound BGTX resonances. A portion of the ROESY spectrum of the 2:1 mixture of BGTX and the α185–196 dodecapeptide is shown which corresponds to the 1-D NMR region shown in Figure 1. Exchange cross-peaks between free and bound BGTX are depicted, and the corresponding chemical shifts (δ) for the free and bound forms of two identified resonances are given.

BGTX Resonance Assignments from Exchange Spectra. As approximately 30% of BGTX resonances were shifted from their free chemical shift position upon binding the dodecapeptide (see below), it was not possible for us to translate directly all the previously determined free BGTX resonance assignments (Basus et al., 1988) to the complex. As shown in Figure 2, however, we observed that, in a 2:1 molar mixture of BGTX and the dodecapeptide where half the BGTX is free and half is bound, there are two sets of BGTX resonances of equal intensity; one set derived from free BGTX and the other set of resonances from bound BGTX. The continual exchange of BGTX between the free and bound states *in the 2:1 mixture* creates additional, non-NOE-related cross-peaks in a standard NOESY spectrum which are due to direct magnetization transfer (i.e., exchange) between homologous pairs of protons in the two distinct slow-exchange conformers of BGTX (Jeener et al., 1979; Meier et al., 1979).

We found that the exchange-related cross-peaks produced in the 2:1 mixture (BGTX/dodecapeptide) provide a powerful tool for rapidly identifying and assigning residues in BGTX that are markedly perturbed upon formation of the complex with the dodecapeptide. Furthermore, this approach may be of general utility in determining the structure of other protein complexes. Figure 2, therefore, illustrates our general strategy in using the chemical-exchange cross-peaks produced in a 2:1 mixture of BGTX/dodecapeptide to assign BGTX resonances in the complex whose chemical shifts are greatly perturbed upon binding. This figure shows a portion of a 2-D ROESY plot corresponding in spectral region to that portrayed in the one-dimensional NMR spectrum of Figure 1. The broad, upfield resonance in Figure 1 (1:1 mixture) corresponds to the broad exchange cross-peak in Figure 2 (BGTX/dodecapeptide, 2:1) which is symmetrically located off the diagonal in the upper right quadrant of the plot. This exchange cross-peak has chemical shift "x–y coordinates" of δ = 6.23 and 6.09 and indicates that one of these two chemical shifts is assignable to a proton in free BGTX and that the other chemical shift must be due to the same proton in the bound conformer of BGTX. The results in the 1-D experiment of Figure 1 argue that the resonance with a δ = 6.23 is that of the bound proton as it is found in the 1:1 complex but it is not present in the BGTX spectrum. From our assignments of proton chemical shifts in free BGTX, the only possibility for the chemical shift at δ = 6.09 is the CαH proton of Met-27. The broadness of this resonance is consistent with the observed behavior of the CαH proton resonance of Met-27 under a variety of conditions in free BGTX, and thus we can assign the resonance at δ = 6.09 to that of the CαH proton of Met-27 in the bound form of BGTX. Similarly, the cross-peak close to the diagonal near the center of the ROESY plot (Figure 2) involving the CδH resonance of His-4 in free BGTX indicates that this resonance is shifted upfield slightly in bound BGTX (δ = 6.33). Finally, the new resonance appearing in the downfield vicinity of the CδH of His-4 in BGTX (see Figure 1) can now be seen to be due to a large upfield shift in the position of the resonance for the CδH proton of His-68 in BGTX (Figure 2). From our assignments of free BGTX at pH 5.8, the His-68 CδH proton has a chemical shift of δ = 6.76 in free BGTX and can thus be assigned to a δ = 6.44 in bound BGTX.

BGTX Residues Perturbed upon Binding. We were able to assign nearly all of the proton resonances of BGTX in the complex using either the ROESY spectra as described above or by comparison with the spectra of free BGTX when the chemical shift changes were too small to observe the exchange cross-peaks. A selected summary of the free and bound resonance assignments is shown in Table I and includes only those residues in BGTX that have resonances which shift dramatically upon binding ($\Delta\delta > 0.15$ ppm). As the resolution of the NOESY spectra is about 0.01 ppm in these experiments, the 0.15 ppm cutoff is somewhat arbitrary but restricts immediate attention to those 16 residues in BGTX with the largest changes in chemical environment upon binding. A schematic highlighting the positions of these 16 amino acids in the molecular model of BGTX is shown in Figure 3. Except for His-68, all the highly perturbed residues are either in the N-terminal loop or in the middle loop (loop II). In addition, however, 11 other residues in BGTX exhibited smaller but significant chemical shift perturbations, in the range of 0.04–0.14 ppm (His-4, Thr-5, Glu-20, Lys-26, Met-27, Cys-33, Gly-43, Tyr-54, Glu-56, Val-57, and Asp-63). Assignments are lacking for only six BGTX residues in the complex: Ser-9 (at the tip of loop I), Ser-34 and Ser-35 (at the end of loop II), and Lys-70, Arg-71 and Gln-72 (in the C-terminal tail segment). All other resonances of BGTX in the complex were minimally perturbed, being within 0.04 ppm of the chemical shift found for free BGTX. Thus, approximately one-third (27 of 74) of the residues in BGTX experience some change in their chemical environment upon complex formation with the dodecapeptide. The β-sheet involving loops II and III is not disrupted by binding as all the diagnostic interstrand NOEs observed in free BGTX (Basus et al.,1988) are retained in bound BGTX.

Dodecapeptide Resonance Assignments. The exchange cross-peak strategy used to assign the resonances of bound BGTX could not be applied to bound dodecapeptide because we could not prepare a 2:1 mixture of dodecapeptide/BGTX due to the limiting solubility of the free peptide at pH 5.8. Instead, the peptide assignments, shown in Table II, were obtained by using the sequential assignment procedure developed by Wüthrich and co-workers (Wüthrich, 1986).

Table I: Comparison of Free and Bound Chemical Shifts for BGTX Residues Perturbed upon Binding[a]

residue		free δ (ppm)	bound δ (ppm)
Thr-6	NH	***8.25***	***8.62***
	αH	4.75	4.79
	βH	***5.03***	***5.69***
	γMe	***1.44***	***1.27***
Ala-7	NH	9.20	9.23
	αH	***4.33***	***4.52***
	βMe	1.54	1.42
Thr-8	NH	***7.06***	***7.43***
	αH	***4.05***	***4.68***
	βH	4.29	4.27
	γMe	1.04	1.06
Pro-10	αH	4.87	4.80
	βH	***2.51***	***2.05***
	β′H	***2.52***	***2.18***
Ile-11	NH	***8.41***	***8.85***
	αH	***4.14***	***3.95***
	βH	***1.69***	***1.50***
	γH	***1.20***	***1.37***
	δMe	***0.91***	***0.25***
	γMe	1.05	0.91
Trp-28	NH	***8.57***	***8.16***
	αH	5.24	5.20
	β′H	3.46	3.44
	βH	3.72	3.79
	NεH	10.50	10.51
	Cδ[1]H	7.03	7.07
	Cε[3]H	7.19	7.16
	Cζ[3]H	7.27	7.35
	CηH	6.87	6.81
	Cζ[2]H	7.54	7.57
Cys-29	NH	***9.37***	***9.55***
	αH	***5.14***	***5.39***
	βH	3.06	3.06
	β′H	3.40	3.48
Asp-30	NH	***8.31***	***9.40***
	αH	4.87	4.99
	βH	2.71	2.75
	β′H	***3.26***	***3.56***
Ala-31	NH	***8.27***	***8.11***
	αH	4.04	4.08
	βMe	1.06	1.06
Phe-32	NH	***8.31***	***8.82***
	αH	4.83	4.83
	βH	***3.44***	***3.10***
	β′H	2.96	2.86
	δH	7.25	7.29
	ζH	7.31	7.35
Gly-37	NH	***7.69***	***7.25***
	αH	***4.35***	***4.58***
	αH	3.91	3.78
Lys-38	NH	***8.16***	***7.81***
Val-39	NH	8.58	8.71
	αH	***3.58***	***3.79***
	βH	***0.36***	***0.14***
	γMe	0.55	0.51
	γ′Me	0.47	0.33
Val-40	NH	***7.59***	***8.11***
	αH	4.68	4.56
	βH	***1.73***	***1.51***
	γMe	0.55	0.55
	γ′Me	0.52	0.49
Glu-41	NH	***9.44***	***9.21***
	αH	5.07	5.07
	βH	***2.28***	***2.08***
	β′H	2.35	2.40
His-68	NH	8.39	8.34
	αH	***4.09***	***3.90***
	βH	2.87	2.82
	β′H	2.78	2.67
	CεH	***7.76***	***8.16***
	CδH	***6.76***	***6.44***

[a] Chemical shifts in bold italic underline indicate BGTX protons whose resonances are shifted by greater than 0.15 ppm upon complex formation.

Strong sequential αH(i), NH(i + 1) as well as βH(i), NH(i + 1) NOESY cross-peaks led to the assignment of residues

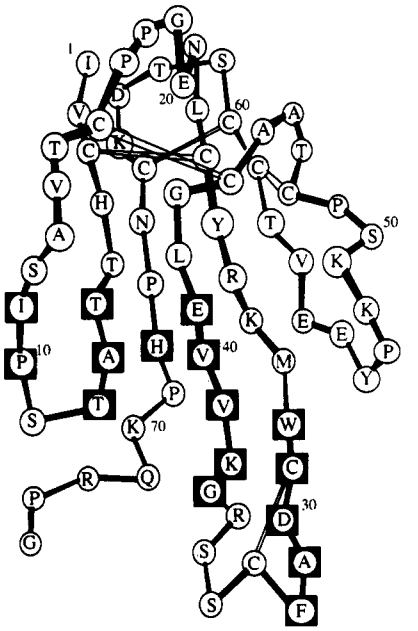

FIGURE 3: Schematic diagram of the BGTX structure. Boxed residues indicate those amino acids whose chemical shifts changed by more than 0.15 ppm upon binding of the α185–196 dodecapeptide. The N-terminal loop is on the left, and disulfide bonds are indicated by the double sets of connecting lines.

Table II: ^{1}H Chemical Shifts[a] and Assignments for the α185–196 Dodecapeptide Complexed to α-Bungarotoxin at 35 °C and pH 5.8

residue	NH	CαH	CβH	others
Lys-185	NA[b]	*c*	*c*	*c*
His-186	*c*	4.74	3.29, 3.09	Cδ^{2}H 7.78; Cε^{1}H 8.11
Trp-187	8.79	4.47	3.19, 3.30	Cε^{3}H 7.65; Cδ^{1}H 7.01; Nε^{1}H 9.65; Cη^{2}H;[c] Cζ^{3}H;[c] Cζ^{2}H[c]
Val-188	8.22	4.08	1.96	Cγ,γ′H$_3$ 1.06, 0.68
Tyr-189	7.85	4.85	2.79, 3.15	Cε^{1}H 6.91; Cδ^{1}H 7.31
Tyr-190	9.31	5.40	2.87, 3.33	Cε^{2}H 6.95; Cδ^{2}H 7.01
Thr-191	*c*	4.17	4.25	CγH$_3$ 1.19
Cys-192	*c*	*c*	*c*	
Cys-193	7.42	5.34	3.38, 3.62	
Pro-194	NA	3.74	*c*	Cδ^{2}H$_2$ 3.31, 3.94; CγH$_2$[c]
Asp-195	8.20	4.73	2.84, 2.52	
Thr-196	7.73	4.08	4.19	CγH$_3$ 1.12

[a] Chemical shifts in ppm from internal 3-(trimethylsilyl)propionate; accuracy ±0.01 ppm. [b] Not applicable. [c] Not assigned.

186–190, 195, and 196. These strong NOEs in the peptide are suggestive of an extended, β-sheet-like conformation in the 186–190 region. Similarly, αH(i), δH(i + 1) and βH(i), δH(i + 1) NOESY cross-peaks helped assign Cys-193 and Pro-194. Although no sequential NOESY cross-peaks were observed for Thr-191, its resonances were identified as the only remaining unassigned Thr spin system in the complex. We were not able, however, to assign the resonances of Cys-192 and Lys-185. Significantly, no NOEs were observed between sequential, NH(i), NH(i + 1), amide protons of the dodecapeptide. Together with the strong sequential αH to NH NOEs typical of β-structure and the several βH to NH sequential NOEs, these results clearly indicate an extended conformation for all of the assigned residues in the dodecapeptide (Table II).

Intermolecular Constraints to the Contact Zone. The combined assignments for BGTX and dodecapeptide proton resonances in the complex enabled us to identify several, structure-delimiting, intermolecular NOESY cross-peaks. The set of intermolecular NOEs listed in Table III define ten BGTX residues and five dodecapeptide residues within the contact zone and include BGTX residues in loops I (Thr-5, Thr-6,

Table III: Pairs of Intermolecular NOEs Defining Contacts between the α185–196 Dodecapeptide and α-Bungarotoxin

dodecapeptide residue	dodecapeptide proton		α-bungarotoxin residue and proton
His-186	CαH	↔	Ala-7 CβH_3
	CβHs	↔	Thr-6 CβH; Ala-7 CαH
	CεH	↔	Thr-5 CαH; Ala-7 CβH; Tyr-24 CεH; Gly-43 NH, CαHs
Trp-187	CδH	↔	Thr-6 CβH
Val-188	CαH	↔	Val-39 Cγ′H_3
	CβH	↔	Val-39 Cγ′H_3; Val-40 Cγ′H_3
	Cγ′H_3	↔	Val-39 CγH_3, Cγ′H_3
	CγH_3	↔	Val-39 Cγ′H_3
Tyr-189	CδHs	↔	Thr-6 CβH; Ile-11 CδH_3; His-68 CδH
	CεHs	↔	Ile-11 NH; Thr-6 CβH; Ile-11 CδH_3; His-68 CδH
Tyr-190	CαH	↔	His-68 CδH
	CβHs	↔	His-68 CδH
	CδHs	↔	Asp-30 NH

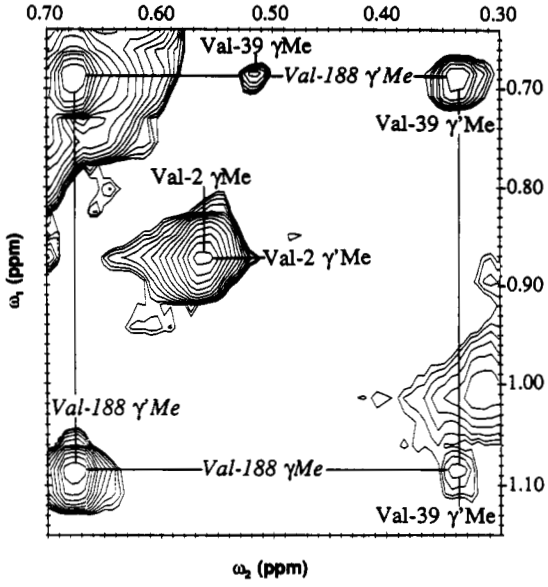

FIGURE 4: A portion of a 2-D NOESY spectrum highlighting intramolecular and intermolecular Val–Val interactions. The 2-D contour plot of the NOESY spectrum reveals the expected strong intramolecular interaction between the two branched Cγ-methyls within a Val residue (e.g., Val-2 of BGTX and Val-188 of the dodecapeptide). The three additional labeled NOE cross-peaks in this region indicate intermolecular interactions between the two Cγ-methyls of Val-39 in BGTX and the two Cγ-methyls of Val-188 in the dodecapeptide.

Ala-7, Ile-11) and II (Tyr-24, Asp-30, Val-39, Val-40, Gly-43) as well as one residue in the C-terminal tail region of BGTX (His-68). Except for Tyr-24, all BGTX residues in the contact zone had some resonances perturbed by greater than 0.04 ppm. Figure 4 illustrates the observed intermolecular NOE cross-peaks between Val-188 of the peptide and Val-39 in BGTX. For comparison, Figure 4 also shows the expected intraresidue NOE cross-peak between the two Cγ-methyls in the side chain of Val-188 (lower left quadrant). The relatively large NOE cross-peak in the upper right quadrant of Figure 4 is due to the strong NOE interaction between one of the Cγ-methyls of Val-188 and the Cγ′-methyl protons of BGTX residue Val-39.

The interproton distance constraints from Table III were then incorporated into a distance geometry algorithm to solve for protein conformations compatible with the distance and chirality restraints. For the distance geometry calculation, the intermolecular distances were set at 5.00 Å as an upper bound only with the addition of the appropriate pseudoatom corrections (Wüthrich, 1986). To simplify the calculations, only the first six amino acids (185–190) of the dodecapeptide were incorporated into the structure of the complex. This was appropriate as no intermolecular NOEs and no long-range intramolecular NOEs were assigned involving peptide residues 191–196. Four representative structures produced by the distance geometry calculation were then further refined by restrained molecular dynamics calculations, and one of the four energy-minimized structures for the complex is shown in Figure 5 (in stereoview). The orientation of BGTX is the same as that in Figure 3. The peptide residues (yellow) corresponding to amino acids KHWVYY are in an extended conformation at a slight angle relative to the plane of the triple-stranded β-sheet in BGTX. The imidazole ring of αHis-186 is at the top-most position overlying Gly-43 and projecting forward. The phenyl ring of Tyr-190 is at the bottom-most position, beneath Lys-38 and projecting to the rear.

DISCUSSION

The Contact Zone between BGTX and the α185–196 Dodecapeptide. The "contact zone" residues of the dodecapeptide are located in the "arm pit" of BGTX created by the N-terminal loop I and middle loop II with His-68 in the C-terminal tail forming a floor to the binding cleft. As shown in Figure 5, the BGTX residues colored in orange represent the combined results of Tables I and III and define the regions in BGTX most strongly affected by interaction with the receptor dodecapeptide. The NOEs between the αHis-186 side chain and the phenyl ring of Tyr-24 in BGTX suggest a hydrogen bond between these two side chains. Stabilizing hydrophobic interactions in the complex are suggested by the proximity of the side chain of Val-188 of the dodecapeptide with side-chain methyls of Val-39 and Val-40 in BGTX (Table III). Likewise, the proximity of the Tyr-189 side chain of the dodecapeptide and Ile-11 of BGTX suggests a possible hydrophobic interaction between these two residues. The large upfield shift of the Ile-11 CδH_3 by 0.66 ppm in the complex (Table I) is consistent with the localization of Ile-11 CδH_3 near the aromatic ring of Tyr-189 as depicted in Figure 5.

The contribution of Tyr-189 and Tyr-190 to the contact zone is consistent with BGTX binding studies using peptide analogues altered at these positions (Gotti et al., 1988; Pearce et al., 1990; Tzartos & Remoundos, 1990). Functional studies involving site-directed mutagenesis also have shown that Tyr-190 plays an important role in the acetylcholine binding site (Tomaselli et al., 1991; Galzi et al., 1991a; O'Leary & White, 1992). Although the conservative replacement of Tyr-190 with Phe in heterologously expressed mouse AChR has little effect on steady state BGTX binding (Tomaselli et al., 1991), presumably because of the multipoint contacts required for BGTX binding and the minimal structural alteration of a Tyr → Phe substitution, the corresponding change in the neuronal α_7 receptor does indeed lead to a detectable decrease in BGTX affinity (Galzi et al., 1991a).

The involvement of loop II residues in BGTX binding to the receptor/dodecapeptide is not surprising as many workers have suggested that loop II is a component of the receptor recognition site and may form an acetylcholine-mimetic structure (Tsernoglou & Petsko, 1976; Ménez et al., 1982; Harvey et al., 1984; Endo & Tamiya, 1987). The involvement of His-68 and loop I (residues 3–16) in BGTX binding to the AChR was not previously predicted although it has been observed that nearly all α-neurotoxins contain either a Ser or a Thr at position 8 in loop I and there is evidence for a functional role of loop I residues in the related short α-neurotoxins (Ménez et al., 1982; Harvey et al., 1984). Recent site-directed

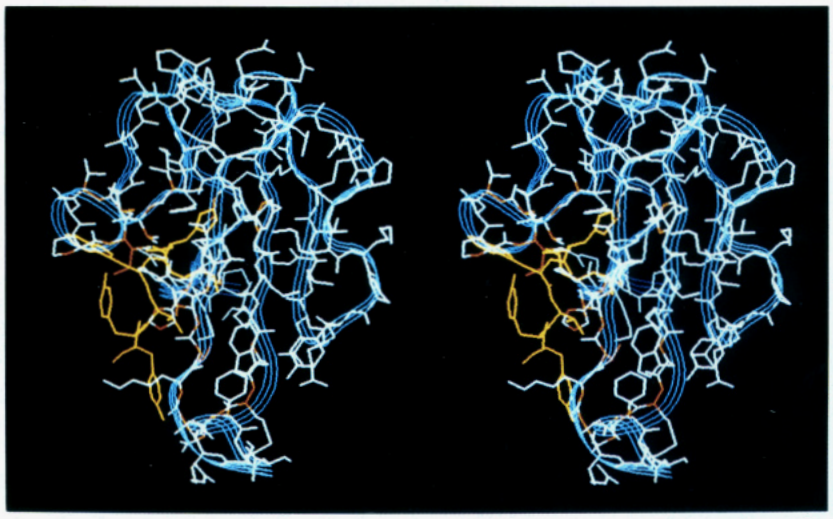

FIGURE 5: Stereoview of the solution structure of BGTX bound to the first six amino acids of the α185–196 dodecapeptide. The tristranded ribbon indicates the position of the BGTX peptide backbone. The peptide residues (KHWVYY) are shown in yellow within the arm pit created between the N-terminal loop I (on left) and the middle loop II. Shown in orange are BGTX atoms whose directly bonded protons undergo a large change in chemical environment ($\Delta\delta \geq 0.15$ ppm as listed in Table I) or which give rise to intermolecular NOESY cross-peaks (Table III).

mutagenesis of recombinant erabutoxin reveals that mutating Ser-8 to a Gly produces a 176-fold decrease in erabutoxin binding to the nAChR (Pillet et al., 1993) consistent with the results reported here. Residues in loop III have also been suggested to participate in receptor recognition (Low et al., 1976; Ménez et al., 1982; Endo & Tamiya, 1987) by forming, with residues from loop II, a concave surface which interacts with the receptor surface. Apart from Tyr-24, we found little indication that binding of the dodecapeptide involves the concave surface directly. Loop III in BGTX may still be important in binding to native receptor if receptor residues other than those contained in the dodecapeptide interact with loop III. It has also been suggested that loops II and III form a cleft into which a receptor Trp residue, either Trp-184 or Trp-187 of the α-subunit, can fit tightly (Low & Corfield, 1987). Our structural data would indicate, however, that the Trp-187 side chain is instead turned toward the bottom end of loop I (Figure 5). The localization of Trp-187 shown in Figure 5 is consistent with fluorescence resonance energy-transfer experiments which suggest a minimal distance in the BGTX/dodecapeptide complex of ~12 Å between Trp-187 of the dodecapeptide and Trp-28 in BGTX (Pearce & Hawrot, 1990).

Conformation of Bound Dodecapeptide. The solution structure of the complex (Figure 5) suggests that the secondary structure of the dodecapeptide involves an extended backbone, as would be found in a β-sheet, at least for amino acids α186–190. A pairwise comparison of the independently calculated structures indicates that the peptide backbone for residues 185–190 in the complex shows an average root mean square deviation of 1.7 Å. The observed extended structure is consistent with the β-sheet secondary structure predicted for residues 184–200 (Stroud et al., 1990) and with circular dichroism studies of the BGTX/dodecapeptide complex which indicate an increase in total β-sheet-like structure upon binding (Shi et al., 1988; Shi and Hawrot, manuscript in preparation).

Conformation of Bound BGTX. Although the overall global structure of BGTX is not drastically disrupted by the binding of the dodecapeptide, there is, nevertheless, significant movement of BGTX residues in a region adjacent to the contact zone. A new intramolecular NOESY cross-peak between Val-39 NH and the NH of Trp-28 in bound BGTX is absent in free BGTX. The proximity of these two NH protons on the opposite strands of loop II in the bound conformation of BGTX indicates that the β-sheet of loop II is being extended downward by one more pair of residues upon binding. This conclusion is further supported by the observation of a second new NOE cross-peak between the CαH of Cys-29 and the NH of Val-39 as expected if the two strands were being zipped together in this region.

The observation of the multipoint NOEs between the CεH of His-186 in the peptide and the αH of Thr-5, the β-methyl of Ala-7, the CεH protons of Tyr-24, and the NH and α-protons of Gly-43 in BGTX is incompatible with the proposed X-ray crystal structure of BGTX (Love & Stroud, 1986). The solution structure of BGTX derived from NMR studies, however, is different from the X-ray structure (Basus et al., 1988), and the preliminary solution structure of free BGTX (V. J. Basus, manuscript in preparation) is completely consistent with the intermolecular NOEs observed in this study.

Contribution of the Dodecapeptide Sequence in BGTX Binding to Native Receptor. There are two lines of argument which suggest that the dodecapeptide sequence may contribute approximately half of the total receptor surface area in contact with BGTX. In the first case we compare the number of amino acid residues involved in the BGTX/dodecapeptide contact zone with the total number of residues involved in several antigen/antibody complexes with binding affinities ($K_d \approx 10^{-10}$ M) comparable to that of BGTX binding to native receptor. X-ray crystallographic studies indicate that contact zones for antigen/antibody complexes typically involve a total of 30–40 amino acids being contributed by the two proteins in the complex (Janin et al., 1990). As we observe a total of 15 amino acids (five from the peptide and ten from BGTX) in close contact in the BGTX/dodecapeptide complex (Table III), we estimate that close to half of the entire native receptor/BGTX contact zone may be represented in the α185–196 dodecapeptide/BGTX complex. The second line of argument comes from calculations based on equilibrium binding constants with the one assumption that the intrinsic binding energy (ΔG) is directly proportional to the surface area of contact with BGTX. From $\Delta G = -RT \ln K_{eq}$, if the dodecapeptide contributes one-half of the total contact surface utilized in BGTX binding to the native receptor, then the K_d for BGTX binding to the dodecapeptide should be the square root of the K_d of BGTX binding to native receptor (i.e., $\sqrt{10^{-11}}$ M or 3×10^{-6} M). The observed K_d of $(1.4–3) \times 10^{-6}$ M (Pearce et al., 1990; Pearce & Hawrot, 1990; this study) is consistent

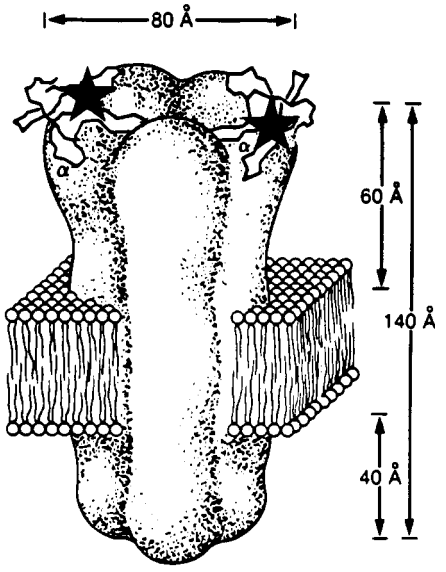

FIGURE 6: Structure of the nicotinic acetylcholine receptor with bound α-neurotoxin. The receptor consists of a pentameric array of subunits with the two α-subunits separated by another subunit. The synaptic surface is located above the membrane bilayer in this representation adapted from Pratt and Taylor (1990) and based on the work of Brisson and Unwin (1985). The backbone structures of two α-neurotoxin molecules are shown atop the α-subunits with loop II projecting into the central well. The approximate position of His-186 in the α-subunit, based on the BGTX/dodecapeptide NMR structure, is indicated by the large star (★).

with half of the total contact surface in the BGTX/receptor complex being represented in the BGTX/dodecapeptide complex. Longer peptide fragments, such as the 18-mer (α181–198) which binds with yet higher affinity (e.g., 6.5×10^{-8} M) (Pearce et al., 1990), should contain more than half of the contact surface utilized in BGTX binding to native receptor.

Location of α186–190 Residues in the Receptor Structure. A number of studies indicate that BGTX lies atop the synaptic ridge of the extracellular portion of the AChR and that loop II may extend partly into the central well of the receptor (Kistler et al., 1982; Fairclough et al., 1983; Johnson et al., 1984; Herz et al., 1987; Kubalek et al., 1987) as illustrated in Figure 6. The observed intermolecular contacts (Table III) suggest that residues 186–190 are located in the outer extracellular half of the native receptor. Assuming that the 40 Å long axis of BGTX is oriented radially down the central well of the receptor, His-186, for example, can be no more than 20 Å from the outer cusp of the receptor and no closer than 40 Å from where the receptor meets the extracellular surface of the membrane bilayer (Figure 6). This localization of residues 186–190 to the extracellular portion of the receptor is contrary to a receptor model that proposes an unusual transmembrane region involving α-subunit residues 179–192 (Pedersen et al., 1990). This latter model is based on immunochemical evidence that residues α156–179 are localized to the cytoplasmic region of the α-subunit. Our findings suggest, however, that His-186 is at least 40 Å from the membrane surface as indicated by the star (★) in Figure 6. The localization of His-186 some 20 Å from the synaptic ridge would place Tyr-190, which is functionally involved in acetylcholine binding (Tomaselli et al., 1991), about 30 Å from the bottom of the central well of the receptor. Our results are therefore consistent with fluorescence energy-transfer experiments with agonist analogues, suggesting that the agonist binding site is located some 30 Å above the base of the central well (Herz et al., 1989). The extracellular localization of Tyr-190 is also supported by the photoaffinity labeling of Tyr-190 with the competitive antagonist DDF (Dennis et al., 1988; Galzi et al., 1990), with [^{3}H]curare (Chiara & Cohen, 1992), and with [^{3}H]nicotine (Middleton & Cohen, 1991).

These studies form a solid base from which we plan to examine complexes formed with longer segments of the α-subunit which should provide more information on the structures involved in macromolecular recognition. We are currently analyzing the 2-D NMR structure of the higher affinity complex formed between BGTX and an 18-mer (α181–198). We also are testing our predictions of contact zone residues by site-directed mutagenesis of an active recombinant BGTX expressed in *Escherichia coli* (Usselman et al., 1993).

ACKNOWLEDGMENT

Additional computational resources were provided by the Computer Graphics Laboratory at UCSF and the San Diego Supercomputer Center. We thank Dr. I. D. Kuntz for helpful discussions and encouragement and for the use of NMR facilities supported by NIH (RR01695), Dr. John Thomason for his modified distance geometry program, Dr. W. van Gunsteren for the GROMOS molecular dynamics program, and Dr. David Busath for use of the Brown University Molecular Graphics Facility.

REFERENCES

Agard, D. A., & Stroud, R. M. (1987) *Acta Crystallogr. A38*, 186–194.

Barchan, D., Kachalsky, S., Neumann, D., Vogel, Z., Ovadia, M., Kochva, E., & Fuchs, S. (1992) *Proc. Natl. Acad. Sci. U.S.A. 89*, 7717–7721.

Basus, V. J., Billeter, M., Love, R. A., Stroud, R. M., & Kuntz, I. D. (1988) *Biochemistry 27*, 2763–2771.

Bax, A., & Davis, D. G. (1985) *J. Magn. Reson. 65*, 355–360.

Betzel, C., Lange, G., Pal, G. P., Wislon, K. S., Maelicke, A., & Saenger, W. (1991) *J. Biol. Chem. 266*, 21530–21536.

Bothner-By, A. A., Stephens, R. L., & Lee, J. (1984) *J. Am. Chem. Soc. 106*, 811–813.

Brisson, A., & Unwin, P. N. T. (1985) *Nature 315*, 474–477.

Changeux, J.-P., Devillers-Thiery, A., Galzi, J.-L., & Bertrand, D. (1992) *Trends Pharmacol. Sci. 13*, 299–301.

Chaturvedi, V., Donnelly-Roberts, D. L., & Lentz, T. L. (1992) *Biochemistry 31*, 1370–1375.

Chiara, D. C., & Cohen, J. B. (1992) *Biophys. J. 61*, 106a.

Conti-Tronconi, B. M., Tang, F., Diethelm, B. M., Spencer, S. R., Reinhardt-Maelicke, S., & Maelicke, A. (1990) *Biochemistry 29*, 6221–6230.

Conti-Tronconi, B. M., Diethelm, B. M., Wu, X., Tang, F., Bertazzon, T., Schroder, B., Reinhardt-Maelicke, S., & Maelicke, A. (1991) *Biochemistry 30*, 2575–2584.

Corfield, P. W. R., Lee, T.-J., & Low, B. W. (1989) *J. Biol. Chem. 264*, 9239–9242.

Dennis, M., Giraudat, J., Kotzyba-Hibert, F., Goeldner, M., Hirth, C., Chang, J. Y., Lazure, C., Chretien, M., & Changeux, J.-P. (1988) *Biochemistry 27*, 2346–2357.

Ellman, G. L. (1959) *Arch. Biochem. Biophys. 82*, 70–77.

Endo, T., & Tamiya, N. (1987) *Pharmacol. Ther. 34*, 403–451.

Endo, T., Inagaki, F., Hayashi, K., & Miyazawa, T. (1981) *Eur. J. Biochem. 120*, 117–124.

Fairclough, R. H., Finer-Moore, J., Love, R. A., Kristofferson, D., Desmeules, P. J., & Stroud, R. M. (1983) *Cold Spring Harbor Symp. Quant. Biol. 48*, 9–20.

Fraenkel, Y., Navon, G., Aronheim, A., & Gershoni, J. M. (1990) *Biochemistry 29*, 2617–2622.

Galzi, J.-L., Revah, F., Black, D., Goeldner, M., Hirth, C., & Changeux, J.-P. (1990) *J. Biol. Chem. 265*, 10430–10437.

Galzi, J.-L., Bertrand, D., Devillers-Thiery, A., Revah, F., Bertrand, S., & Changeux, J.-P. (1991a) *FEBS Lett. 294*, 198–202.

Galzi, J.-L., Revah, F., Bessis, A., & Changeux, J.-P. (1991b) *Annu. Rev. Pharmacol. 31*, 37–72.
Gippert, G. P., Ping, F. Y., Wright, P. E., & Case, D. A. (1990) *Biochem. Pharmacol. 40*, 15–22.
Gotti, C., Mazzola, G., Longhi, R., Fornasari, D., & Clementi, F. (1987) *Neurosci. Lett. 82*, 113–119.
Gotti, C., Frigerio, F., Bolognesi, M., Longhi, R., Racchetti, G., & Clementi, F. (1988) *FEBS Lett. 228*, 118–122.
Gray, W. R., Luque, F. A., Galyean, R., Atherton, E., Sheppard, R. C., Stone, B. L., Reyes, A., Alford, J., McIntosh, M., Olivera, B. M., Cruz, L. J., & Rivier, J. (1984) *Biochemistry 23*, 2796–2802.
Hamilton, S. L., Pratt, D. R., & Eaton, D. C. (1985) *Biochemistry 24*, 2210–2219.
Harvey, A. L., Hider, R. C., Hodges, S. J., & Joubert, F. J. (1984) *Br. J. Pharmacol. 82*, 709–716.
Havel, T. F., Crippen, G. M., & Kuntz, I. D. (1979) *Biopolymers 18*, 73–81.
Herz, J. M., Johnson, D. A., & Taylor, P. (1987) *J. Biol. Chem. 262*, 7238–7247.
Inagaki, F., Hider, R. C., Hodges, S. J., & Drake, A. F. (1985) *J. Mol. Biol. 183*, 575–590.
Janin, J., & Chothia, C. (1990) *J. Biol. Chem. 265*, 16027–16030.
Jeener, J., Meier, B. H., Bachmann, P., & Ernst, R. R. (1979) *J. Chem. Phys. 71*, 4546–4553.
Johnson, D. A., Voet, J. G., & Taylor, P. (1984) *J. Biol. Chem. 259*, 5717–5725.
Kao, P. N., & Karlin, A. (1986) *J. Biol. Chem. 261*, 8085–8088.
Kao, P. N., Dwork, A. J., Kaldany, R.-R., Silver, M. L., Wideman, J., Stein, S., & Karlin, A. (1984) *J. Biol. Chem. 259*, 11662–11665.
Kistler, J., Stroud, R. M., Klymkowsky, M. W., Lalancette, R. A., & Fairclough, R. H. (1982) *Biophys. J. 37*, 371–383.
Kubalek, E., Ralston, S., Lindstrom, J., & Unwin, N. (1987) *J. Cell Biol. 105*, 9–18.
Kuntz, I. D., Thomason, J. F., & Oshiro, C. M. (1989) in *Methods of Enzymology* (Oppenheimer, N. J., & James, T. L., Eds.) Vol. 177, pp 159–204, Academic Press, Orlando, FL.
Labhardt, A. M., Hunziker-Kwik, E. H., & Wüthrich, K. (1988) *Eur. J. Biochem. 177*, 295–305.
Le Goas, R., LaPlante, S. R., Mikou, A., Delsuc, M.-A., Guittet, E., Robin, M., Charpentier, I., & Lallemand, J.-Y. (1992) *Biochemistry 31*, 4867–4875.
Love, R. A., & Stroud, R. M. (1986) *Protein Eng. 1*, 37–46.
Low, B. W., & Corfield, P. W. R. (1987) *Asia Pac. J. Pharmacol. 2*, 115–127.
Low, B. W., Preston, H. S., Sato, A., Rosen, L. S., Searl, J. E., Rudko, A. D., & Richardson, J. R. (1976) *Proc. Natl. Acad. Sci. U.S.A. 73*, 2991–2994.
McLane, K. E., Wu, X., Diethelm, B., & Conti-Tronconi, B. M. (1991) *Biochemistry 30*, 4925–4934.
Meier, B. H., & Ernst, R. R. (1979) *J. Am. Chem. Soc. 101*, 6441–6442.
Ménez, A., Boulain, J.-C., Faure, G., Couderc, J., Liacopoulos, P., Tamiya, N., & Fromageot, P. (1982) *Toxicon 20*, 95–103.
Middleton, R. E., & Cohen, J. B. (1991) *Biochemistry 30*, 6987–6997.
Mishina, M., Tobimatsu, T., Imoto, K., Tanaka, K., Fujita, Y., Fukuda, K., Kurasaki, M., Takahashi, H., Morimoto, Y., Hirose, T., Inayama, S., Takahashi, T., Kuno, M., & Numa, S. (1985) *Nature 313*, 364–369.
Neumann, D., Barchan, D., Fridkin, M., & Fuchs, S. (1986a) *Proc. Natl. Acad. Sci. U.S.A. 83*, 9250–9253.
Neumann, D., Barchan, D., Safran, A., Gershoni, J. M., & Fuchs, S. (1986b) *Proc. Natl. Acad. Sci. U.S.A. 83*, 3008–3011.
Ohana, B., Fraenkel, Y., Navon, G., & Gershoni, J. M. (1991) *Biochem. Biophys. Res. Commun. 179*, 648–654.
O'Leary, M. E., & White, M. M. (1992) *J. Biol. Chem. 267*, 8360–8365.
Oswald, R. E., Sutcliffe, M. J., Bamberger, M., Loring, R. H., Braswell, E., & Dobson, C. M. (1991) *Biochemistry 30*, 4901–4909.
Pearce, S. F., & Hawrot, E. (1990) *Biochemistry 29*, 10649–10659.
Pearce, S. F. A., Preston-Hurlburt, P., & Hawrot, E. (1990) *Proc. R. Soc. London, B 241*, 207–213.
Pedersen, S. E., Bridgman, P. C., Sharp, S. D., & Cohen, J. B. (1990) *J. Biol. Chem. 265*, 569–581.
Pillet, L., Tremeau, O., Ducancel, F., Drevet, P., Zinn-Justin, S., Pinkasfeld, S., Boulain, J.-C., & Ménez, A. (1993) *J. Biol. Chem. 268*, 909–916.
Pratt, W. B., & Taylor, P. (1990) *Principles of Drug Action*, 836 pp, Churchill Livingstone, New York.
Radding, W., Corfield, P. W. R., Levinson, L. S., Hashim, G. A., & Low, B. W. (1988) *FEBS Lett. 231*, 212–216.
Ralston, S., Sarin, V., Thanh, H. L., Rivier, J., Fox, L., & Lindstrom, J. (1987) *Biochemistry 26*, 3261–3266.
Rivier, J., Kaiser, R., & Galyean, R. (1978) *Biopolymers 17*, 1927–1938.
Shi, Q.-L., Colson, K. L., Lentz, T. L., Armitage, I. M., & Hawrot, E. (1988) *Biophys. J. 53*, 94a.
Stroud, R. M., McCarthy, M. P., & Shuster, M. (1990) *Biochemistry 29*, 11009–11023.
Sutcliffe, M. J., Dobson, C. M., & Oswald, R. E. (1992) *Biochemistry 31*, 2962–2970.
Tomaselli, G. F., McLaughlin, J. T., Jurman, M. E., Hawrot, E., & Yellen, G. (1991) *Biophys. J. 60*, 721–727.
Tsernoglou, D., & Petsko, G. A. (1976) *FEBS Lett. 68*, 1–4.
Tzartos, S. J., & Remoundos, M. S. (1990) *J. Biol. Chem. 265*, 21462–21467.
Usselman, J. A., Hsu, S. H., Messier, N. J., Vaslet, C. A., & Hawrot, E. (1993) *Biophys. J. 64*, A116.
van Gunsteren, W. F., & Berendsen, H. J. C. (1987) *GROMOS Manual*, Biomos b.v. Biomolecular Software, Groningen, The Netherlands.
Walkinshaw, M. D., Saenger, W., & Maelicke, A. (1980) *Proc. Natl. Acad. Sci. U.S.A. 77*, 2400–2404.
Wilson, P. T., Lentz, T. L., & Hawrot, E. (1985) *Proc. Natl. Acad. Sci. U.S.A. 82*, 8790–8794.
Wilson, P. T., Hawrot, E., & Lentz, T. L. (1988) *Mol. Pharmacol. 34*, 643–650.
Wüthrich, K. (1986) *NMR of Proteins and Nucleic Acids*, 292 pp, Wiley, New York.
Yu, C., Lee, C.-S., Chuang, L.-C., Shei, Y.-R., & Wang, C. Y. (1990) *Eur. J. Biochem. 193*, 789–799.
Zinn-Justin, S., Roumestand, C., Gilquin, B., Bontems, F., Ménez, A., & Toma, F. (1992) *Biochemistry 31*, 11335–11347.